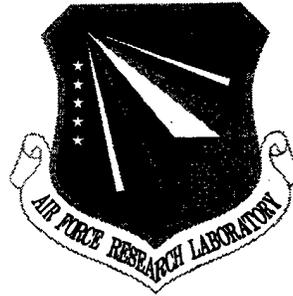RL-TR-97-238
Final Technical Report
March 1998

IMAGING THROUGH FIBERS, PHASE 3

Regents of the University of Michigan

Emmett N. Leith

*APPROVED FOR PUBLIC RELEASE; DISTRIBUTION UNLIMITED.*

19980324 018

DTIC QUALITY INSPECTED

**AIR FORCE RESEARCH LABORATORY
ROME RESEARCH SITE
ROME, NEW YORK**

This report has been reviewed by the Air Force Research Laboratory, Information Directorate, Public Affairs Office (IFOIPA) and is releasable to the National Technical Information Service (NTIS). At NTIS it will be releasable to the general public, including foreign nations.

RL-TR-97-238 has been reviewed and is approved for publication.

APPROVED: *[signature]*

REINHARD K. ERDMANN
Project Engineer

FOR THE DIRECTOR: *[signature]*
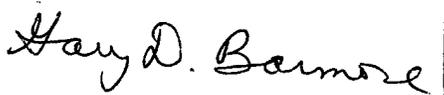
GARY D. BARMORE, Major, USAF
Chief, Rome Operations Office
Sensors Directorate

If your address has changed or if you wish to be removed from the Air Force Research Laboratory mailing list, or if the addressee is no longer employed by your organization, please notify AFRL/SNDP, 25 Electronic Pky, Rome, NY 13441-4515. This will assist us in maintaining a current mailing list.

Do not return copies of this report unless contractual obligations or notices on a specific document require that it be returned.

ALTHOUGH THIS REPORT IS BEING PUBLISHED BY AFRL, THE RESEARCH WAS ACCOMPLISHED BY THE FORMER ROME LABORATORY AND, AS SUCH, APPROVAL SIGNATURES/TITLES REFLECT APPROPRIATE AUTHORITY FOR PUBLICATION AT THAT TIME.

REPORT DOCUMENTATION PAGE

Form Approved
OMB No. 0704-0188

1. AGENCY USE ONLY *(Leave blank)*	2. REPORT DATE March 1998	3. REPORT TYPE AND DATES COVERED Final Feb 96 – Dec 96

4. TITLE AND SUBTITLE
IMAGING THROUGH FIBERS, PHASE 3

5. FUNDING NUMBERS

C - F30602-96-2-0062
PE - 62702F
PR - 4600
TA - P5
WU - PK

6. AUTHOR(S)
Emmett N. Leith

7. PERFORMING ORGANIZATION NAME(S) AND ADDRESS(ES)
Regents of the University of Michigan
3003 South State Street, Room 1058
Ann Arbor MI 48109-1274

8. PERFORMING ORGANIZATION REPORT NUMBER

N/A

9. SPONSORING / MONITORING AGENCY NAME(S) AND ADDRESS(ES)
Air Force Research Laboratory/SNDP
25 Electronic Pky
Rome NY 13441-4515

10. SPONSORING / MONITORING AGENCY REPORT NUMBER

RL-TR-97-238

11. SUPPLEMENTARY NOTES

Air Force Research Laboratory Project Engineer: Reinhard K. Erdmann, SNDP, (315) 330-4455

12a. DISTRIBUTION AVAILABILITY STATEMENT

APPROVED FOR PUBLIC RELEASE; DISTRIBUTION UNLIMITED

12b. DISTRIBUTION CODE

13. ABSTRACT *(Maximum 200 words)*
Direct relay of images over single mode (SM) fiber has been demonstrated by coherence (holographic) methods. For the usual two-dimensional case, the need is eliminated for prior digitization of input images, and no additional fiber coupling is required. Interestingly, the method functions for 3-D images just as well. Experiments carried out in the previous phase of this work demonstrated holographic image transmission over a pair of single mode fibers for the first time. The implementation utilized an available Acousto-Optic (A/O) modulator reference signal relayed over the second SM fiber. This final phase of the project simulates the data rate capabilities of such a system if it were implemented with state of the art A/O cell and detector array technology. A computer stores the device parameters and provides the necessary coherent image processing. The study also details the performance improvements that would result from use of high performance Spatial Light Modulator (SLM) arrays in place of A/O cells for encoding of the reference phase. A 1-D SLM generates 2-D images as does the A/O, whereas a 2-D SLM array permits 3-D imaging. Data rates and signal/noise are analyzed for a wide range of parameters in both configurations. A rate of 4 GHz with a Bit-Error-Rate of 10^{-6} results from a particular SLM 1-D configuration based on existing device technology. A full system would require a second SLM for real time use. On the other hand the much simpler A/O based system would require developmental components to approach even a 1 GHz rate.

14. SUBJECT TERMS
holography, single mode (SM) fiber, coherent processing, optical imaging, spatial light modulator (SLM)

15. NUMBER OF PAGES
28

16. PRICE CODE

17. SECURITY CLASSIFICATION OF REPORT **UNCLASSIFIED**	18. SECURITY CLASSIFICATION OF THIS PAGE **UNCLASSIFIED**	19. SECURITY CLASSIFICATION OF ABSTRACT **UNCLASSIFIED**	20. LIMITATION OF ABSTRACT UL

TABLE OF CONTENTS

FIGURE CAPTIONS

Figure 1   System for transmitting 3-D images through single-mode fiber.

Figure 2   Block diagram for the coherence encoding system, where we have assumed perfect codes with cross-correlations equal to 0 and autocorrelations equal to 1. The A-O implementation looks like a frequency division multiplexing (FDM) system, where the individual f_i functions are single frequency temporal carriers. For the SLM case we have essentially a code division multiplexing (CDM) scheme, where the individual f_i functions are random, pseudo-random, or deterministic phase functions.

Figure 3   A-O case bias photon noise SNR and the quantization noise SNR as a function of N, with fixed exposure (250,000 detected photons per pixel), hence linearly increasing laser power. The detector quantization is assumed to be 8 bit.

Figure 4   Coherence encoding implemented with 2-D phase only SLMs replacing the A-O cells. In this case the SLM is driven by a time varying 2-D function, such that the cross correlation of any two pixels over an adequate amount of time becomes zero. Each pixel on the SLM, being at the back focal plane of a collimating lens, illuminates the object with a single plane wave, and all the plane waves are mutually incoherent due to the modulation described above.

Figure 5   Required laser power as a function of N for the A-O case, with various fixed frame rates, fixed exposure level (250,000 detected photons per pixel), and an object to reference beam ratio of unity at the mixing plane. Also an additional factor of 4 power loss is assumed in the object beam due to the object distribution and stray losses.

Figure 6   Results for an 8x8 binary phase source SLM and 8x8 binary amplitude input SLM using an orthogonal codeword set with codeword length of 64. (a) binary transmittance object; (b) reconstructed 64x64 image; (c) sampled and binarized version of image in Fig. 6(b); (d) image formed using coherent plane wave illumination.

Figure 7   Results for a 16x16 binary phase source SLM and 8x8 binary amplitude input SLM using an orthogonal codeword set with codeword length of 256; (a) reconstructed 64 x 64 image. (b) sampled and binarized version of image in Fig. 7(a).

Figure 8   Results for a 16x16 analog phase source SLM and 8x8 binary amplitude input SLM using a random phase code (uniform from $-\pi$ to π). (a) reconstructed 64 x 64 image for a code of length 256; (b) reconstructed 64x64 image for a code of length 2048.

Introduction

The phase 3 contract called for a continuation of the work on phases 1 & 2. In phase 1, we demonstrated the transmission of an image over a single fiber using the process of holography, with the reference beam propagated over free space. In phase 2 a number of extensions were carry out, the primary on being the demonstration of transmission of an image over a single, single-mode fiber. The task was accomplished, and the results were successful.

Background

The theory was previously demonstrated in the phase 1 contract by transmitting an image over a single 12 micrometer multimode fiber, with a free-space propagated reference beam. In phase 2 we used a single-mode fiber, and we also confined the reference beam to a single fiber. Thus, we have transmitted a complete image, both phase and amplitude, over a pair of single-mode fibers.

The basic idea is explained with the aid of Fig. 1. Light from a monochomatic, spatially incoherent source, generated for instance by running an expanded laser beam through a moving diffuser, illuminates an object. If the illuminating source had been spatially coherent (a single plane wave) then the object Fourier transform would be formed at the back focal plane of lens L_1 (plane P_3). Noting that the entrance end of the fiber is also positioned in plane P_3, and assuming the fiber to be on axis and the illuminating plane wave to be propagating down the z axis, the zero spatial frequency (or DC) component of the Fourier transform would pass through the fiber. Of course, many Fourier components of the Fourier transform would pass through the fiber. However, many Fourier

1

components are required to form an image, and they must all be combined with the proper phase relationships.
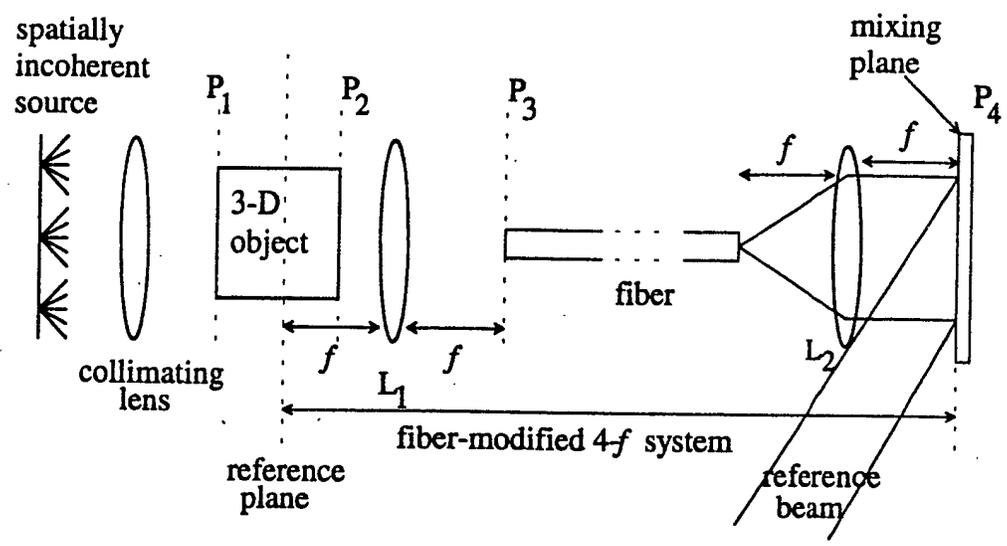
Figure 1 System for transmitting 3-D images through single-mode fiber.

We note that the incoherent source can be viewed as a collection of mutually incoherent plane waves with different spatial frequencies. This becomes evident when we take the diffuser to be a random phase grating. Allowing the diffuser to be stationary, the illuminating plane wave, upon propagation through the diffuser, will generate a continuum of plane waves with a certain phase relationship. As the diffuser moves, the

phase of each individual plane wave will vary with time in a random manner, thereby broadening its temporal bandwidth and making the set of plane waves mutually incoherent, assuming the integration time to be long relative to the diffuser motion.

Now each component plane wave of the incoherent source projects a Fourier transform to plane P_3. The Fourier transforms are displaced from each other in accordance with the spatial frequency of the source plane wave component. Each spatial frequency element thus shifts a different object spatial frequency component to zero, whereby all object spatial frequency components get coupled into the fiber. The object spatial frequencies have been encoded as mutually incoherent temporal waveforms, or coherence elements, and transmitted down the fiber in parallel.

From the above viewpoint, the spatially incoherent source is not strictly monochromatic. However, a source with any degree of spatial incoherence cannot be strictly monochromatic; a strictly monochromatic extended source would have coherence between the different source elements. In the theoretical treatment of spatially incoherent illuminating sources, sufficient bandwidth is required so that over the detection time the correlation between light from different source elements will be zero; but also, the source bandwidth is assumed sufficiently narrow that path differences between the two interfering beams are small compared to the coherence length of the light. A suitable source for the process described here is a He-Ne laser with a coherence length of a few cm. The temporal bandwidth broadening caused by the production of a spatially incoherent source generation method, such as propagating through rotating ground glass, is generally less than the inherent bandwidth of the laser. Hence,

3

the process we describe here of image formation through fibers is properly described in terms of spatial incoherence effects and not on temporal incoherence effects.

In order to recover the image each temporal waveform much be decoded to its corresponding spatial frequency element. To decode the signal, a portion of the laser light is split off from the incident beam before it reaches the object-illuminating diffuser, and is transmitted via another fiber to a plane P_4. Being a monochromatic spatially coherent beam, it can be transmitted through the fiber without distortion. The beam exiting the reference fiber is then sent through a diffuser identical to the object-illuminating diffuser and having the same motion. The spatial and temporal object illumination field is hence reproduced at the receiver end of the reference branch. The two beams are brought together to form a hologram. In the recording process, each spatial frequency element of the reference beam will interfere only with the corresponding temporal waveform exiting the object branch fiber and will create a fringe pattern of the appropriate spatial frequency. The image can then be produced from the hologram by the usual methods, yielding a 3-D complex image.

Objective

The objective of this Phase 3 effect was to analyze and evaluate imaging obtained with the object beam traveling over one fiber and the reference beam traveling over a second fiber.

The Task requirements were as follows:

1.   Analyze and experimentally verify the data rates and signal to noise ratios that are obtainable with the new technique of imaging over a pair of single mode fibers.

2.   Extend the technique to the second lateral dimension. [To date, our experimental results have been for one lateral dimension and the depth dimension.]

3.   Investigate whether the new method can compensate for dispersion over fibers.

4.   Investigate other methods, besides acoustic cells, of providing the spatially incoherent illumination source.

Description of Accomplishments

The greatest part of the effort was on task 1. Task 4 was also carried out. By mutual agreement, task 2 was omitted, since the necessary equipment for doing it was not available. However, simulation of task 2 was carried out. We also looked into task 3 and concluded that the new method was not helpful with the dispersion problem.

An in-depth extensive analysis of the system performance is presented in a paper currently being published. In this final report, we summarize the analysis and state the results. Specifically, performance of the confined reference coherence encoding method for two and three dimensional complex image/data transmission through optical fibers was analyzed. Both Acousto-Optic and phase only spatial light modulator implementations were considered. Signal to noise ratio, data rate, and probability of bit error issues were discussed. Simulation results were presented.

Our coherence imaging method is an optical implementation of a waveform encoder-decoder. It encodes spatial frequencies which the single-mode fiber cannot support into temporal waveforms which the fiber does support. The waveform encoder implemented by this method is a

highly parallel system that automatically transmits complex symbols (amplitude-phase). Figure 2 shows the block diagram for the coherence encoding system, where we have assumed perfect codes with cross-correlations equal to 0 and autocorrelations equal to 1. For a typical A-O system the total number of object components sent in parallel (N) can readily be 1000, a conventional equivalent would therefore require 1000 mixers at the input and 1000 correlators at the output. The system looks like a 1000 channel frequency division multiplexing (FDM) system. For the SLM case we have essentially a code division multiplexing (CDM) scheme. The random, pseudo-random, or deterministic phase modulation at each SLM pixel in time can be viewed as the code for that SLM pixel and hence for the associated object spatial frequency component. For a typical SLM size of 128 squared this systems yields 16384 parallel channels.
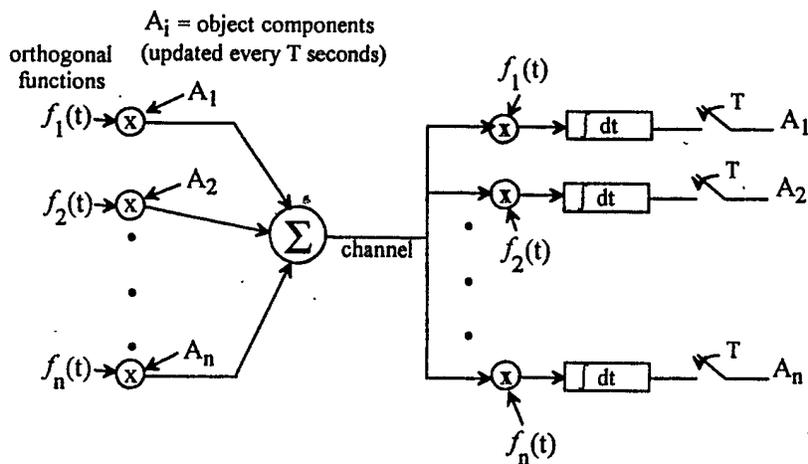

Fig. '2 Block diagram for the coherence encoding system, where we have assumed perfect codes with cross-correlations equal to 0 and autocorrelations equal to 1. The A-O implemetation looks like a frequency division multiplexing (FDM) system, where the individual f_i functions are single frequency temporal carriers. For the SLM case we have essentially a code division multiplexing (CDM) scheme, where the individual f_i functions are random, psuedo-random, or deterministic phase functions.

The maximum data rate, in pixels per second, achievable by the A-O system described here is determined by the bandwidth (W) of the A-O cells. Driving the A-O cells as described above, we can simultaneously generate up to N resolvable spatial frequencies and hence send up N object spatial frequency components in parallel (where N is the number of resolvable spots of the A-O cells). In order for the N resolvable spatial frequencies to be incoherent (independent) we require a minimum detector integration time of N/W, the inverse of the spectral separation of two adjacent A-O resolvable spots, yielding a data rate of W complex (magnitude and phase) spatial frequency components per sec. A-O cells with a bandwidth (W) of 1 GHz are readily available.

In the 2-D SLM case we send N pixels in parallel, where $N^{1/2}$ is the number of SLM pixels along one dimension and the SLM is assumed to be square. The minimum integration time is the codeword length for each pixel (L) divided by the frame rate (W) of the SLM. For simplicity we assume the use of a binary phase (0 or π) SLM, limiting ourselves to binary codes. If an orthogonal codeword set is used, the length of each codeword (L) is N and the data rate becomes W.

We next consider an analog SLM where each pixel is modulated by a random phase function (uniformly distributed from $-\pi$ to π) in time. This type of modulation is akin to the original rotating diffuser implementation previously described. In this case the cross correlation fringe patterns can be found to have energy proportional to $1/L^{1/2}$, where L is the number of phase changes over the integration time and the energy is normalized to the autocorrelation fringe pattern energy. The SNR, due to a single cross-correlation term, is therefore $L^{1/2}$; however, all N-1 pixels will add crosstalk energy to any given pixel, making the total crosstalk SNR much

7

lower. Considering the f_O object spatial frequency term, assuming the phase of the object spatial frequency distribution to be uniformly distributed from $-\pi$ to π, and ignoring the reference beam spatial carrier, we see that the autocorrelation term will create a fringe pattern of spatial frequency f_O and that each crosstalk term will add a low contrast fringe pattern with spatial frequency f_O and randomized phase. The crosstalk fringe energy will build as $(N-1)^{1/2}$ (or approximately $N^{1/2}$), since the individual crosstalk terms are randomly phased, yielding a total crosstalk SNR of $(L/N)^{1/2}$. For the analog SLM case setting L equal to N yields a crosstalk SNR of only 1 whereas for the binary SLM case setting L equal to N allows the complete elimination of crosstalk, assuming the binary phase modulator is perfect. Clearly using structured coherence encoding (the binary phase SLM method) is more efficient in terms of required integration time versus attained decorrelation than is the random phase method (rotating diffuser) previously described.

Although the number of pixels sent in parallel can be very high with a 2-D SLM, the overall data rate is still rather low due to the low frame rates of currently commercially available SLMs (typically 1 KHz to 10 KHz for ferroelectric devices). Translating this to transmitted image frame rate based on 128 squared pixel SLM, we get results of only ~0.6 frames/s. Multiple quantum well devices, however, have been used to generate SLMs with modulation speeds on the order of 5 GHz. These devices can be optically addressed and phase modulation has been demonstrated. Furthermore, MQW devices have been successfully integrated with silicon based electronics and large arrays (128x128) with 100 KHz frames rates have been demonstrated.

The data rates discussed above consider only the modulator-channel-demodulator portion of the system. In a full system we must also consider presenting the input data and decoding the output data which is in the form of a hologram or interferogram. Presenting the data in real time via another SLM yields a more general data transmission system. From the general data transmission point of view the 1-D A-O implementation remains attractive.

For the A-O case, considering a high end 1 GHz A-O with 1000 point resolution, we see that to achieve the 1 GHz data rate we must be able to update the input data and decode the output data in 1 ms (1 MHz). Since the A-O based system works in one dimension only we simply require a 1-D input device and a 1-D detector in the mixing plane. The input data could be presented using a linear SLM array. Nematic liquid crystal (NLC) devices, which switch at ~10 ms, would be much too slow for this application. Significantly faster ferroelectric liquid crystal (FLC) devices could also be used; these devices switch at ~10 ms which is still a factor of 10 slower than would be required to achieve the A-O modulator/demodulator based data rate. Alternatively, multiple-quantum-well (MQW) devices could be used, allowing the A-O based data rate to be achieved. Also, MQW SLM devices can be optically addressed.

In order to decode $N=1000$ pixels from the recorded hologram/interferogram made up of 1000 transmitted spatial frequency components we require at least a 4000 pixel linear array detector. The factor of 4 is due to the spatial carrier required by holography. The detected signal must be decoded via a Fourier transformation, spatial filtering, inverse Fourier transformation process. This could be done digitally by reading out the array and processing it using dedicated

9

hardware or digital signal processor (DSP) hardware. If the data is to be decoded digitally it is advantageous to have the array size be a power of 2, therefore, for the case above we assume the detector array to be 4096 pixels long. In conventional linescan arrays the image array charge is quickly transferred to a buffer array from where it is actually read out. In order to achieve the 1 GHz data rate based on the A-O bandwidth this charge transfer time should be insignificant relative to the integration time (<< 1 ms). In currently available linescan devices this transfer time is < 100 ns, meeting the requirement for A-O limited data rate. Also, to achieve the A-O limited data rate, we require the read out and decoding time to be less than or equal to the integration time. Dividing the time equally between the two processes, we see that we require a read out rate on the order of 8 GHz. Currently available 8 tap linescan arrays can achieve read out/digitization rates of ~120 MHz. The required read out rate could theoretically be achieved by going to 512 taps; however with commercially available devices we would clearly currently be limited by the array read out rate if the A-O modulation bandwidth exceeded ~15 MHz. A typical A-O resolution (N) at 15 MHz would be 100 points.

If we were able to read out and digitize the array in the allotted 0.5 ms based on the 1 GHz A-O case, the information would still have to be decoded in 0.5 ms. This could be done using dedicated fast Fourier transform (FFT) hardware. A more general approach would be to use digital signal processors (DSP). Using a real valued input optimized radix-2 FFT algorithm, we would require a processing throughput of ~60 GFLOPS to decode the data in 0.5 ms; clearly this would require a parallel DSP approach (~256 *Butterfly DSP Inc.* BDSP9124 60 MHz DSPs). In the read

out rate limited case, assuming a 100 point resolution 15 MHz bandwidth A-O, we would require ~1.5 GFLOPS of processing throughput (~8 DSPs).

The dedicated FFT hardware approach mentioned above could also be implemented in the same substrate as the linear CCD array. In this case the final read out rate could be reduced by a factor of 4 since the decoded image, having 1/4 as many pixels as the recorded interferogram, is read out instead of the interferogram. For a detected 4096 pixel interferogram and a radix-16 implementation this would require 6 stages of processing; $\log_{16}(4096)$ stages for the forward FFT and $\log_{16}(4096)$ for the inverse FFT.

Another approach could be to read out the linear CCD array in analog form and use it to drive an A-O cell or an SLM linear array which could be used as the input device to an optical Fourier processor decoder (simply a 4-f spatial filtering system). If the A-O input optical decoder method is used we require an A-O device with 4 times more bandwidth than the modulator/demodulator A-Os, due to the increased bandwidth of the recorded interferometric signal. In this case the total system throughput would be limited to 1/4 the bandwidth of the optical Fourier processor input A-O device, assuming we are not detector read out limited. Similarly, if NLC or FLC SLM devices were to be used as the optical Fourier processor system input, the total system data rate would be limited by the decoder portion of the system; however, if MQW devices were to be used the system data rate could again be A-O modulator/demodulator or detector read out time limited. Another option could be to use an optically addressed MQW SLM device directly as the detector and the optical Fourier processor input.

Returning to the 2-D SLM modulator/demodulator system, considering 128x128 FLC binary phase SLMs operating at 10 KHz, and utilizing a full orthogonal code, we see that in order to achieve the modulator/demodulator SLM limited data rate of 10 KHz we would need to refresh the input image and decode the output hologram in ~1.6 s. Clearly this is not a problem in either case. For the input image, either NLC or FLC devices could be used. For the 128x128 2-D modulator/demodulator case we need to record the interferogram using at least a 128x512 CCD (the spatial carrier is only required along one dimension). Reading out the array at 1 MHz would require ~100 ms and the FFT processing could readily be performed in <100 ms using a single DSP. These methods would also be adequate at 100 KHz modulator/demodulator frame rates but faster processing and read out rates would be required in the 1 MHz or higher regime. The solutions discussed for the A-O case could also be applied here.

Signal to noise ratio

Using the results in the previous section, along with the analysis developed previously, expressions for the SNR have been developed. The analysis is somewhat lengthy to give here, but will appear in a paper to be published.

An example of the SNR results is shown in Fig. 3, a plot of an equation for the SNR based on typical parameters, e.g., a CCD well depth of 300,000 electrons, wavelength of 1.3 microns, a pixel size of 10 micons squared. The figure shows the SNR as a function of N, the number of frequency components in the signal. Both the photon-limited SNR and the quantization-limited SNR are shown. The bias photon noise induced SNR is clearly the dominant term.
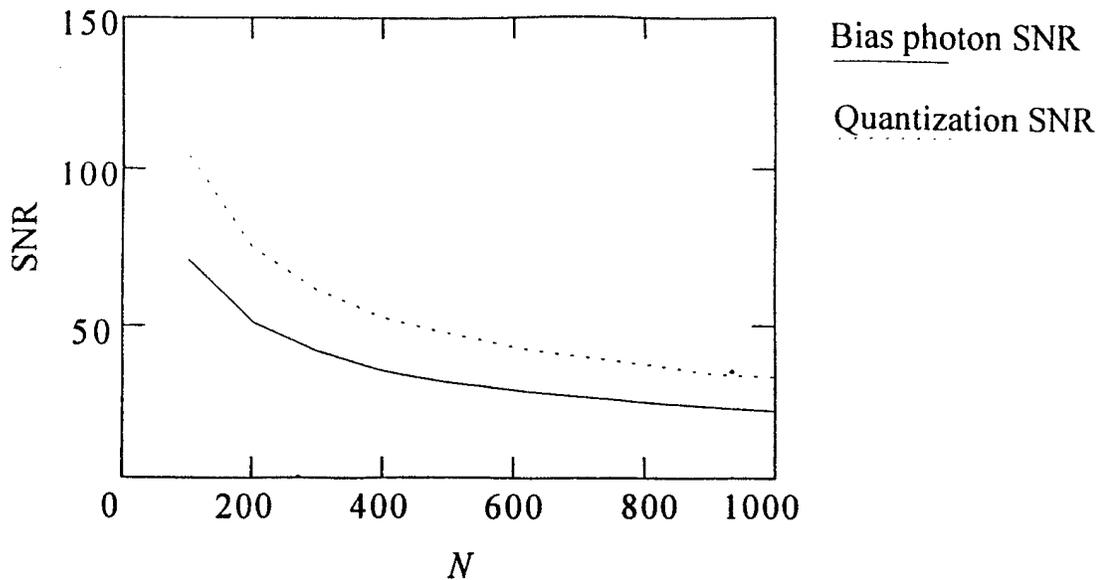
12

Fig. 3 A-O case bias photon noise SNR and the quantization noise SNR as a function of N, with fixed exposure (250,000 detected photons per pixel), hence linearly increasing laser power. The detector quantization is assumed to be 8 bit.

Also the probability of bit error rate was analyzed. The analysis is several pages long and is not given here; it is included in the paper to be published. The results are given as equations and as graphs that give bit error rate as a function of the various relevant parameters, such as data rate, number of frequency components in the signal, input power, etc. For example, it was found that with 225 mW of input power, data rates of 4 GHz with a probability of bit error of 10^{-6} are achieved. Finally, since the implementation of a system with 2 dimensions of lateral resolution was not carried out, the result was simulated. The simulations is for a 2-D spatial light modulator and is based on physical optics and the thin optical element approximation, where optical elements are represented by planar transmittance functions. The simulation calculates the coherent interferogram for each realization of the illumination SLM and adds the set of interferograms incoherently simulating the CCD integration process. For each realization, the illumination source is modeled as a summation of

13

plane waves traveling in different directions and having phase shifts determined by the source SLM. The object transmittance is then multiplied by this coherent, spatially random, illumination and the Fourier transform present in plane P_1 is calculated. The single-mode fiber is simply modeled as a low-pass spatial filter and the object field at the mixing plane is calculated. The coherent spatially broad illumination is then placed on a spatial carrier and added to the object field at the mixing plane. The detected coherent interferogram is calculated by taking the intensity of the total field at the mixing plane. This process is repeated for many realizations of the coherent spatially broad illumination and the total spatially incoherent interferogram is calculated. Image reconstruction (decoding) proceeds as if the interferogram had been obtained experimentally.
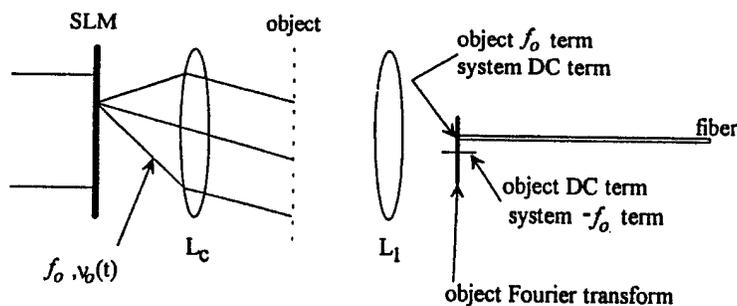
Fig. 4. Coherence encoding implemented with 2-D phase only SLMs replacing the A-O cells. In this case the SLM is driven by a time varying 2-D function, such that the cross correlation of any two pixels over an adequate amount of time becomes zero. Each pixel on the SLM, being at the back focal plane of a collimating lens, illuminates the object with a single plane wave, and all the plane waves are mutually incoherent due to the modulation described above.

The first simulation uses an 8x8 point binary amplitude random object. The object is made up of square pixels having a pixel pitch equal to the pixel size. The illumination source is made up of 8x8 spatial frequency elements, centered about zero spatial frequency and having a cutoff frequency corresponding to the pixel pitch of the object. These spatial frequency components are generated by an 8x8 binary phase SLM at the back focal plane of a collimating lens (Fig. 4). A 64-bit binary orthogonal codeword set is used to drive the 64 source SLM pixels. This is the maximum data rate configuration. The 64 coherent realizations are calculated and summed incoherently yielding the incoherent interferogram having zero crosstalk between the individual object spatial frequency components. Figure 5(a) shows the object and Fig. 5(b) shows the reconstructed image at 1/4 the detector resolution (64x64). We are limited to 1/4 of the detector resolution in the reconstructed image due to the spatial carrier required by interferometric recording. The reconstructed image is then sampled and binarized, generating the 8x8 image in Fig. 5(c). Figure 5(d) shows how the system performs under coherent illumination (a collimated plane wave). In this case the reconstructed image is simply the point spread function caused by the fiber aperture, or alternatively is made up of only the dc spatial frequency component of the object; hence, no imaging occurs.
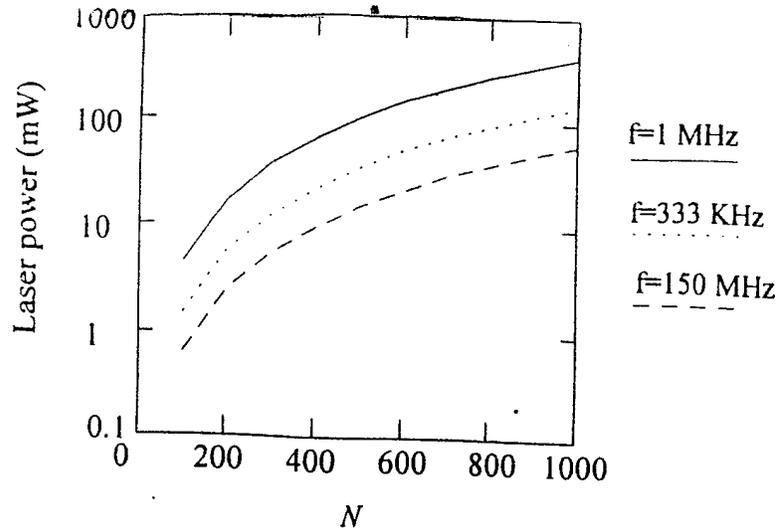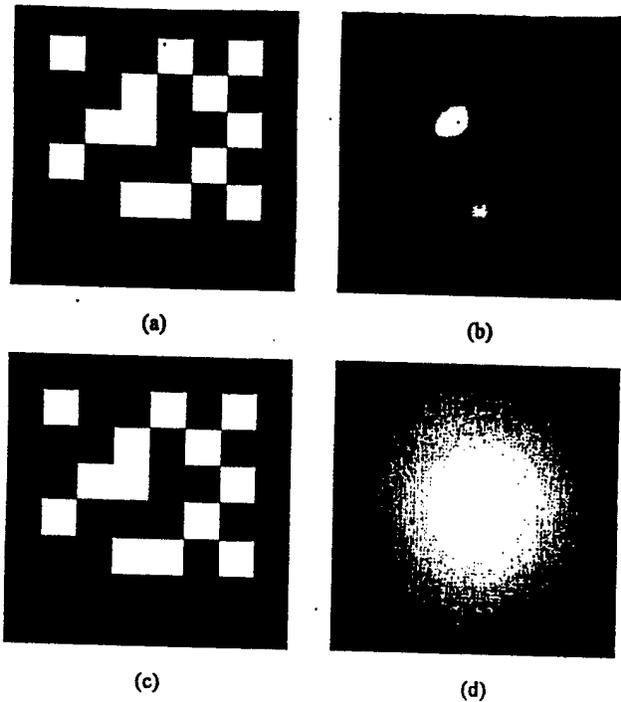
(a)

(b)

(c)

(d)

Fig. 6 Results for an 8x8 binary phase source SLM and 8x8 binary amplitude input SLM using an orthgonal codeword set with codeword length of 64. (a) binary transmittance object. (b) reconstructed 64x64 image. (c) sampled and binarized version of image in Fig. 6(b). (d) image formed using coherent plane wave illumination.

    Although the final image is perfect [Fig. 6(c)] and there is no spatial frequency crosstalk, we see intersymbol interference (ISI) in Fig. 6b) caused by a combination of the 100% fill factor object and the minimal source spatial bandwidth cutoff (corresponding to the object pixel pitch).

This ISI makes the system susceptible to noise. ISI can be eliminated in various ways, including shaping the individual object pixels or increasing the illumination spatial bandwidth. Assuming an input SLM is being used to generate the object distribution, both these methods amount to having higher resolution SLMs. In the second simulation we reduce ISI by increasing the illumination spatial frequency cutoff to twice that corresponding to the object pixel pitch and increasing the number of component plane waves to 16x16. The code length was also increased to 256 bits; maintaining orthogonality of all the illumination plane waves. Figure 7(a) shows the 64x64 reconstructed image, the ISI is significantly reduced. Figure 7(b) shows the sampled and binarized image.
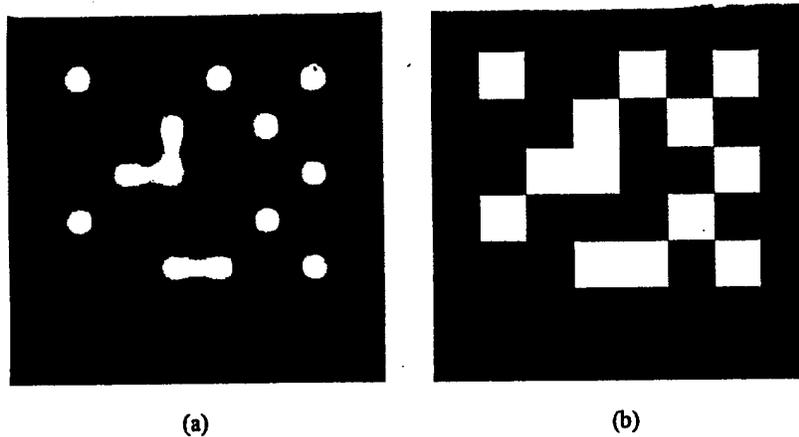

(a)   (b)

Fig. 7   Results for a 16x16 binary phase source SLM and 8x8 binary amplitude input SLM using an orthgonal codeword set with codeword length of 256. (a) reconstructed 64x64 image. (b) sampled and binarized version of image in Fig. 7(a).
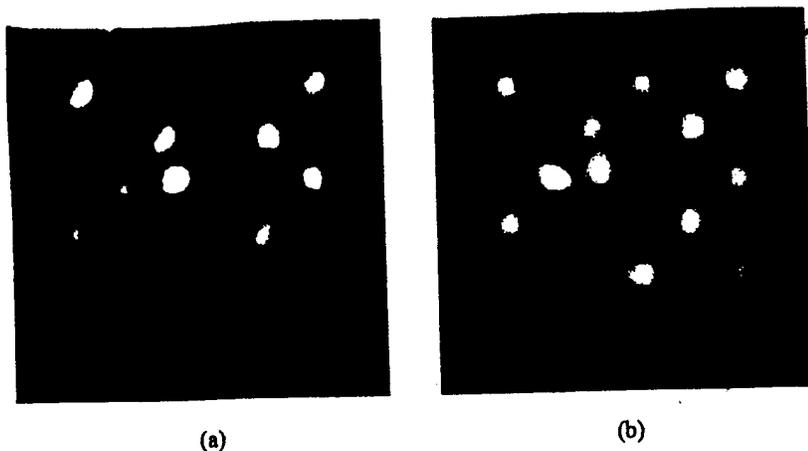
(a)   (b)

Fig. 8   Results for a 16x16 analog phase source SLM and 8x8 binary amplitude input SLM using a random phase code (uniform from -π to π). (a) Reconstructed 64x64 image for a code of length 256. (b) Reconstructed 64x64 image for a code of length 2048.

Figure 8 shows the results using an analog phase source SLM driven randomly generating random phase uniformly distributed from -π to π. As in Fig. 7, the source SLM size is set to 16x16 (low ISI configuration). Figure 8(a) shows the reconstructed 64x64 image for a code length of 256. As described above we expect a spatial frequency crosstalk SNR of 1. Although it is difficult to quantify the crosstalk SNR seen in Fig. 8(a) it is clearly significantly worse than the equal length binary code case [Fig. 7(a)]. Figure 8(b) shows the reconstructed 64x64 image for a code length of 2048. The image still looks worse than the 256 length binary code case.

The simulations described above were also run using phase objects, yielding similar results.